

See discussions, stats, and author profiles for this publication at: <https://www.researchgate.net/publication/5274334>

Cinnamoyl Inhibitors of Tissue Transglutaminase †

ARTICLE *in* THE JOURNAL OF ORGANIC CHEMISTRY · JULY 2008

Impact Factor: 4.72 · DOI: 10.1021/jo8004843 · Source: PubMed

CITATIONS

39

READS

54

4 AUTHORS, INCLUDING:



Joelle N Pelletier

Université de Montréal

77 PUBLICATIONS 1,685 CITATIONS

SEE PROFILE



Jeffrey Keillor

University of Ottawa

84 PUBLICATIONS 1,356 CITATIONS

SEE PROFILE

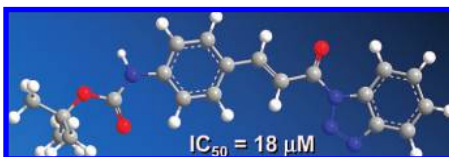
Cinnamoyl Inhibitors of Tissue Transglutaminase[†]

Christophe Pardin, Joelle N. Pelletier, William D. Lubell, and Jeffrey W. Keillor*

Département de chimie, Université de Montréal, C.P. 6128, Succursale centre-ville, Montréal, Québec H3C 3J7, Canada

jw.keillor@umontreal.ca

Received March 4, 2008



Transglutaminases (TGases) catalyze the intermolecular cross-linking of certain proteins and tissue TGases (TG2) are involved in diverse biological processes. Unregulated, high TGase activities have been implicated in several physiological disorders, but few reversible inhibitors of TG2 have been reported. Herein, we report the synthesis of a series of novel *trans*-cinnamoyl derivatives, discovered to be potent inhibitors of guinea pig liver transglutaminase. The most effective inhibitors evaluated can be sorted into two subclasses: substituted cinnamoyl benzotriazolyl amides and the 3-(substituted cinnamoyl)pyridines, referred to more commonly as azachalcones. Kinetic evaluation of both of these subclasses revealed that they display reversible inhibition and are competitive with acyl donor TGase substrates at IC_{50} values as low as $18\ \mu\text{M}$. An analysis of structure–activity relationships within these series of inhibitors permitted the identification of potentially important binding interactions. Further testing of some of the most potent inhibitors demonstrated their selectivity for TG2 and their potential for further development.

Introduction

Transglutaminases (TGases, EC 2.3.2.13) are calcium-dependent enzymes that catalyze the intermolecular cross-linking of certain proteins through the formation of γ -glutamyl- ϵ -lysine side chain to side chain bridges (Scheme 1). In mammals, three types of TGases displaying this activity have been characterized to date and are found in tissue, plasma, and epidermis. Tissue TGases are involved in diverse biological processes such as endocytosis,^{1,2} apoptosis,³ and cell growth regulation.⁴ The plasma-soluble form of TGase, Factor XIIIa, stabilizes blood

clots by catalyzing the cross-linking of fibrin during hemostasis.^{5,6} Epidermal TGase plays a key role in the synthesis of the cornified envelope of epidermal keratinocytes.⁷

Unregulated, high TGase activities have been implicated in physiological disorders involved in disease states such as acne,⁸ cataracts,⁹ immune system diseases,¹⁰ psoriasis,¹¹ Alzheimer's

[†] Abbreviations used: BOC, *tert*-butoxycarbonyl; Cbz, benzyloxycarbonyl; DIC, diisopropylcarbodiimide; DMAP, 4-(dimethylamino)pyridine; DMF, dimethylformamide; DMSO, dimethyl sulfoxide; Fmoc, 9-fluorenylmethoxycarbonyl; GDH, glutamate dehydrogenase; IC_{50} , concentration of inhibitor necessary to reduce enzyme activity to half of that observed in the absence of inhibitor; KHMDS, potassium bis(trimethylsilyl)amide; β -NADH, β -nicotinamide adenine dinucleotide; TFA, trifluoroacetic acid; TGase, transglutaminase; TG2, tissue transglutaminase; THF, tetrahydrofuran.

(1) Levitzki, A.; Willingham, M.; Pastan, I. H. Evidence for participation of transglutaminase in receptor-mediated endocytosis. *Proc. Natl. Acad. Sci. U.S.A.* **1980**, *77*, 2706–2710.

(2) Davies, P. J.; Davies, D. R.; Levitzki, A.; Maxfield, F. R.; Milhaud, P.; Willingham, M. C.; Pastan, I. H. Transglutaminase is essential in receptor-mediated endocytosis of α 2-macroglobulin and polypeptide hormones. *Nature (London)* **1980**, *283*, 162–167.

(3) Fesus, L.; Thomazy, V.; Falus, A. Induction and activation of tissue transglutaminase during programmed cell death. *FEBS Lett.* **1987**, *224*, 104–108.

(4) Birckbichler, P. J.; Orr, G. R.; Patterson, M. K.; Conway, E.; Carter, H. A.; Maxwell, M. D. Enhanced transglutaminase activity in transformed human lung fibroblast cells after exposure to sodium butyrate. *Biochim. Biophys. Acta* **1983**, *763*, 27–34.

(5) Lorand, L. Fibrinolytic: the fibrin-stabilizing factor system of blood plasma. *Ann. N.Y. Acad. Sci.* **1972**, *202*, 6–30.

(6) Pisano, J. J.; Finlayson, J. S.; Peyton, M. P. Cross-link in Fibrin Polymerized by Factor XIII: ϵ -(γ -Glutamyl)lysine. *Science* **1968**, *160*, 892–893.

(7) Candi, E.; Tarcsa, E.; Digiovanna, J. J.; Compton, J. G.; Elias, P. M.; Marekov, L. N.; Steinert, P. M. A highly conserved lysine residue on the head domain of type II keratins is essential for the attachment of keratin intermediate filaments to the cornified cell envelope through isopeptide crosslinking by transglutaminases. *Proc. Natl. Acad. Sci. U.S.A.* **1998**, *95*, 2067–2072.

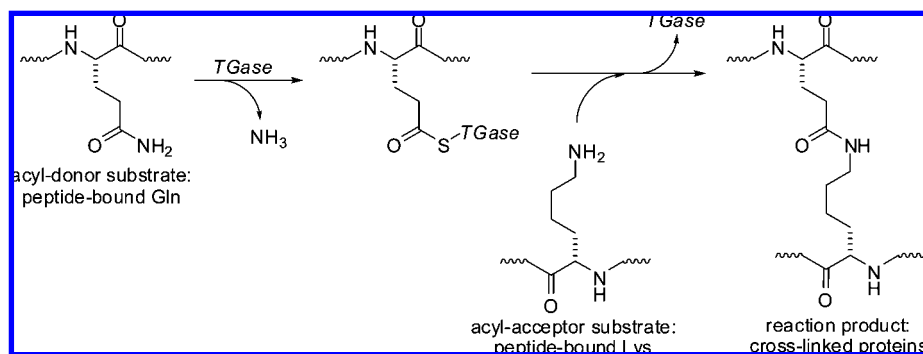
(8) De Young, L.; Ballaron, S.; Epstein, W. Transglutaminase Activity in Human and Rabbit Ear Comedogenesis: A Histochemical Study. *J. Invest. Dermatol.* **1984**, *82*, 275–279.

(9) Azari, P.; Rahim, J.; Clarkson, D. P. Transglutaminase activity in normal and hereditary cataractous rat lens and its partial purification. *Curr. Eye Res.* **1981**, *463*–469.

(10) Fesus, L. Transglutaminase activation: significance with respect to immunologic phenomena. *Surv. Immunol. Res.* **1982**, *1*, 297–304.

(11) Schroeder, W. T.; Thatcher, S. M.; Stewart-Galetka, S.; Annarella, M.; Chema, D.; Siciliano, M. J.; Davies, P. J. A.; Tang, H. Y.; Sowa, B. A.; Duvic, M. Type I Keratinocyte Transglutaminase: Expression in Human Skin and Psoriasis. *J. Invest. Dermatol.* **1992**, *99*, 27–34.

SCHEME 1. TGase-Mediated Protein Cross-Linking



disease,^{12,13} Huntington's disease,^{14,15} Celiac disease,¹⁶ and cancer metastasis.^{17,18} Potent and selective TGase inhibitors offer means for elucidating the roles of TGases in various disease states and may serve as lead compounds for therapeutic development.

In recent years TGase activity has been shown to be regulated by a number of potential TGase inactivators, including sulfonamides,^{19,20} iodoacetates^{21–24} (i.e., iodoacetamide (**1**)), isocyanates²⁵ (e.g., propyl isocyanate (**2**)), thioureas²⁶ (e.g., 1-(5-aminopentyl)-3-phenylthiourea (**3**)), acivicin derivatives^{27,28} (e.g., benzyl 1-((3-bromo-4,5-dihydroisoxazol-5-yl)methylcarbamoyl)-2-phenylethylcarbamate (**4**)), sulfonium methyl ke-

tones,²⁹ thioacetyl heterocycles³⁰ (e.g., 1,4,5-trimethyl-2-[(2-oxopropyl)thio]imidazole (**5**)), and electrophilic glutamine analogues³¹ (Figure 1). Poor selectivity has, however, limited the therapeutic utility of these classes of inhibitors. Improved affinity for TGase has been displayed by irreversible inhibitors such as dipeptide-bound 1,2,4-thiadiazoles³² (e.g., *N*_α-carbobenzyl-2-amino-*N*_δ-(3-methyl-5-[1,2,4]thiadiazolyl)-L-glutamine (**6**)), α,β-unsaturated amides,³³ and epoxides³³ (e.g., *N*_α-carbobenzyl-2-amino-*N*_ω-acryloyl-L-lysylglycine (**7d**) and *N*_α-carbobenzyl-2-amino-*N*_ω-oxiranecarbonylamino-L-lysylglycine (**7h**); Figure 2). These inhibitors are generally selective for tissue TGase, in comparison to microbial TGase or γ-glutamyl transpeptidase (GGT), a related transpeptidase.³⁴

Thieno[2,3-*d*]pyrimidin-4-one acylhydrazide derivatives have recently been reported³⁵ to be reversible and potent inhibitors of tissue transglutaminase (TG2). An initial structure–activity relationship study for this class of TG2 inhibitors revealed that the acylhydrazide thioether side chain was important for affinity. Analogues bearing a thiophene ring, such as the thieno[2,3-*d*]pyrimidin-4-one acylhydrazide derivatives **8a–c** (Figure 3) were among the most potent inhibitors and exhibited slow-binding inhibition.

In our previous studies of structural elements required for TG2 substrate recognition, we remarked upon the distinctive

(12) Selkoe, D. J.; Abraham, C.; Ihara, Y. Brain Transglutaminase: In vitro Crosslinking of Human Neurofilament Proteins into Insoluble Polymers. *Proc. Natl. Acad. Sci. U.S.A.* **1982**, *79*, 6070–6074.

(13) Norlund, M. A.; Lee, J. M.; Zainelli, G. M.; Muma, N. A. Elevated transglutaminase-induced bonds in PHF tau in Alzheimer's disease. *Brain Res.* **1999**, *851*, 154–163.

(14) Dedeoglu, A.; Kubilus, J. K.; Jeitner, T. M.; Matson, S. A.; Bogdanov, M.; Kowall, N. W.; Matson, W. R.; Cooper, A. J. L.; Ratan, R. R.; Beal, M. F. Therapeutic Effects of Cystamine in a Murine Model of Huntington's Disease. *J. Neurosci.* **2002**, *22*, 8942–8950.

(15) Mastroberardino, P. G.; Iannicola, C.; Nardacci, R.; Bernassola, F.; De Laurenzi, V.; Melino, G.; Moreno, S.; Pavone, F.; Oliverio, S.; Fesus, L. 'Tissue' transglutaminase ablation reduces neuronal death and prolongs survival in a mouse model of Huntington's disease. *Cell Death Differ.* **2002**, *9*, 873–880.

(16) Piper, J. L.; Gray, G. M.; Khosla, C. High Selectivity of Human Tissue Transglutaminase for Immunoactive Gliadin Peptides: Implications for Celiac Sprue. *Biochemistry* **2002**, *41*, 386–393.

(17) Choi, K.; Siegel, M.; Piper, J. L.; Yuan, L.; Cho, E.; Strnad, P.; Omary, B.; Rich, K. M.; Khosla, C. Chemistry and Biology of Dihydroisoxazole Derivatives: Selective Inhibitors of Human Transglutaminase 2. *Chem. Biol.* **2005**, *12*, 469–475.

(18) Keillor, J. W. Tissue Transglutaminase Inhibitors. *Chem. Biol.* **2005**, *12*, 410–412.

(19) Lorand, L.; Rule, N. G.; Ong, H. H.; Furlanetto, R.; Jacobsen, A.; Downey, J.; Oner, N.; Bruner-Lorand, J. Amine specificity in transpeptidation. Inhibition of fibrin cross-linking. *Biochemistry* **1968**, *7*, 1214–1223.

(20) Stenberg, P.; Nilsson, I.; Erickson, O.; Lunden, R. Fibrin-stabilizing factor inhibitors. II. The inhibitory properties of various aliphatic amines. *Acta Pharm. Sued.* **1971**, *8*, 415–422.

(21) Holbrook, J. J.; Cooke, R. D.; Kingston, I. B. The amino acid sequence around the reactive cysteine residue in human plasma Factor XIII. *Biochem. J.* **1973**, *135*, 901–903.

(22) Chung, S. I.; Lewis, M. S.; Folk, J. E. Relationships of the Catalytic Properties of Human Plasma and Platelet Transglutaminases (Activated Blood Coagulation Factor XIII) to Their Subunit Structures. *J. Biol. Chem.* **1974**, *249*, 940–950.

(23) Curtis, C. G.; Brown, K. L.; Credo, R. B.; Domanik, R. A.; Gray, A.; Stenberg, P.; Lorand, L. Calcium-dependent unmasking of active center cysteine during activation of fibrin stabilizing factor. *Biochemistry* **1974**, *13*, 3774–3780.

(24) Folk, J. E.; Finlayson, J. S. The epsilon-(gamma-glutamyl)lysine crosslink and the catalytic role of transglutaminases. *Adv. Protein Chem.* **1977**, *31*, 1–133.

(25) Gross, M.; Whetzel, N. K.; Folk, J. E. Alkyl isocyanates as active site-directed inactivators of guinea pig liver transglutaminase. *J. Biol. Chem.* **1975**, *250*, 7693–7699.

(26) Lee, K. N.; Fesus, L.; Yancey, S. T.; Girard, J. E.; Chung, S. I. Development of selective inhibitors of transglutaminase. Phenylthiourea derivatives. *J. Biol. Chem.* **1985**, *260*, 14689–14694.

(27) Castelano, A. L.; Billedeau, R.; Pliura, D. H.; Bonaventura, B. J.; Krantz, A. Synthesis, chemistry and absolute configuration of novel transglutaminase inhibitors containing a 3-halo-4,5-dihydroisoxazole. *Bioorg. Chem.* **1988**, *16*, 335–340.

(28) Auger, M.; McDermott, A. E.; Robinson, V.; Castelano, A. L.; Billedeau, R. J.; Pliura, D. H.; Krantz, A.; Griffin, R. G. Solid-state ¹³C NMR study of a transglutaminase-inhibitor adduct. *Biochemistry* **1993**, *32*, 3930–3934.

(29) Pliura, D. H.; Bonaventura, B. J.; Pauls, H. W.; Killackey, J. F.; Krantz, A. Irreversible inhibition of transglutaminases by sulfonium methylketones: optimization of specificity and potency with ω-aminoacyl spacers. *J. Enzyme Inhib.* **1992**, *6*, 181–194.

(30) Freund, K. F.; Doshi, K. P.; Gaul, S. L.; Claremon, D. A.; Remy, D. C.; Baldwin, J. J.; Pitzenger, S. M.; Stern, A. M. Transglutaminase inhibition by 2-[(2-oxopropyl)thio]imidazolium derivatives: mechanism of factor XIIIa inactivation. *Biochemistry* **1994**, *33*, 10109–10119.

(31) Doyle, P. M.; Harris, C. J.; Carter, K. R.; Simpkin, D. S. A.; Bailey-Smith, P.; Stone, D.; Russel, L.; Blackwell, G. Peptides incorporating electrophilic glutamine analogues as potential transglutaminase inhibitors. *Biochem. Soc. Trans.* **1990**, *18*, 1318–1320.

(32) Marrano, C.; de Macédo, P.; Gagnon, P.; Lapierre, D.; Gravel, C.; Keillor, J. W. Synthesis and Evaluation of Dipeptide-Bound 1,2,4-Thiadiazoles as Irreversible Transglutaminase Inhibitors. *Bioorg. Med. Chem.* **2001**, *9*, 3231–3241.

(33) Marrano, C.; de Macédo, P.; Keillor, J. W. Evaluation of Novel Dipeptide-Bound α,β-Unsaturated Amides and Epoxides as Irreversible Inhibitors of Guinea Pig Liver Transglutaminase. *Bioorg. Med. Chem.* **2001**, *9*, 1923–1928.

(34) Keillor, J. W.; Lubell, W. D.; Pardin, C. Cinnamoyl Inhibitors of transglutaminase. PCT Int. Appl. filed 29 May 2008 from U.S. Patent 60,940,523.

(35) Duval, E.; Case, A.; Stein, R. L.; Cuny, G. D. Structure-activity relationship study of novel tissue transglutaminase inhibitors. *Bioorg. Med. Chem. Lett.* **2005**, *15*, 1885–1889.

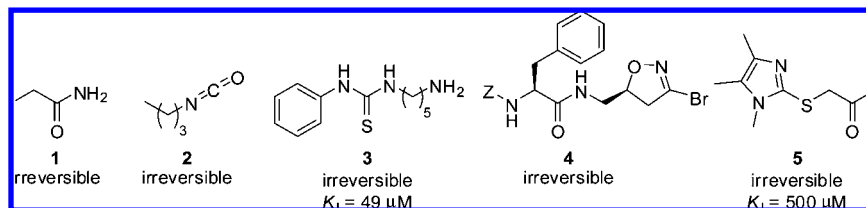


FIGURE 1. Representative structures of transglutaminase inhibitors.^{19–31}

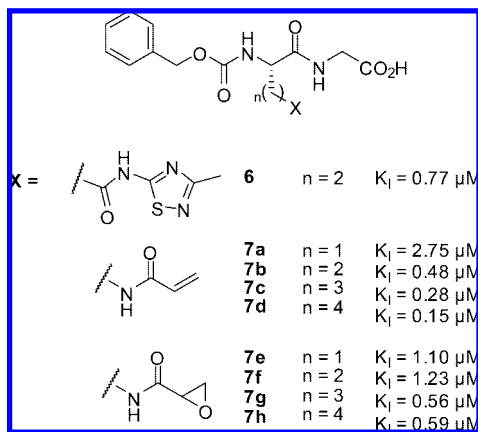


FIGURE 2. Representative structures of specific transglutaminase inhibitors.^{32,33}

ability of the Cbz protecting group to confer improved affinity.³⁶ Investigation of the importance of the rigidity of the Cbz group led to the synthesis and biological evaluation of *trans*-cinnamoyl derivatives, during which some synthetic precursors were found to bind TG2 much more tightly than the target substrate analogues. Cinnamoyl analogues have previously been found to exhibit inhibitory activity on various enzymes and proteins, including the fungal 17 β -hydroxysteroid dehydrogenase³⁷ (**9** and **10**), the integrin α v β 3 receptors³⁸ (**11**), and α -glucosidase³⁹ (**12**) (Figure 4). In pursuit of potent and selective TG2 inhibitors, several series of *trans*-cinnamoyl derivatives have been synthesized and evaluated to provide a better understanding of their structure–activity profiles. The initial structure–activity relationship study of this new class of tissue TGase inhibitors has demonstrated their efficiency as rapid, competitive, and reversible inhibitors with IC₅₀ values as low as 18 μ M.

Results and Discussion

Chemistry. Cinnamoyl benzotriazolyl amides **14a–c,l** and **15a,d–k,m–q** were initially studied as potential TG2 inhibitors. The coupling of various *trans*-cinnamic acid derivatives with benzotriazole and hydroxybenzotriazole was performed using

diisopropylcarbodiimide (DIC) and 4-(dimethylamino)pyridine (DMAP) in dimethylformamide (DMF) overnight at room temperature. Although the resulting product mixture could be purified by diluting in ethyl acetate (EtOAc) and washing successively with NaOH, HCl, and brine, significant amounts of product were lost during the washing steps. For this reason, after removal of the EtOAc phase, the substituted cinnamoyl benzotriazolyl amides were isolated by trituration or by flash column chromatography, in 12–70% isolated yields (Scheme 2). The structure of amide **14a** was confirmed by X-ray crystallographic analysis and showed that N-acylation of the hydroxybenzotriazole moiety had occurred, instead of formation of its ester counterpart (Figure 5). *trans*-Cinnamic acids that were not commercially available were typically prepared in 37–74% yields by the Wittig olefination of the corresponding substituted benzaldehyde with ((*tert*-butoxycarbonyl)methyl)-triphenylphosphonium bromide in tetrahydrofuran (THF) using potassium bis(trimethylsilyl)amide (KHMDS) as a base at room temperature (Scheme 2). Amino-substituted cinnamoyl benzotriazole amides (**15n–p**) were synthesized by reduction of the corresponding nitrocinnamoyl *tert*-butyl ester using tin(II) chloride (SnCl₂) in ethanol.⁴⁰ The crude anilines **13r,s** were acylated with FmocCl or (BOC)₂O to provide the N-protected aminocinnamic acids **13n–p**. These N-protected aminocinnamic acids were used without further purification and treated with benzotriazole under the same coupling conditions as described above (Scheme 3).

Azachalcones **30a,r,t** were synthesized as a second subclass of inhibitor candidates by aldol condensation of different substituted benzaldehydes with 3-acetylpyridine using potassium hydroxide in a 50/50 MeOH/H₂O solution.⁴¹ For example, *p*-nitro-azachalcone **30a** precipitated from the reaction mixture and was obtained in pure form after simple filtration, in 73% yield. *p*-Nitro-azachalcone **30a** was reduced with SnCl₂⁴⁰ to provide *p*-amino-azachalcone **30r**, which was then acetylated with a solution of 40% acetic anhydride/pyridine at room temperature over 1 h (Scheme 4).

For comparison, cinnamate **19a** and cinnamides **18a**, **21a–27a**, and **29a** were synthesized from *p*-nitrocinnamic acid by activation with *p*-nitrophenyl chloroformate, triethylamine, and DMAP in acetonitrile to form ester **17a**, which precipitated.⁴² After filtration and washing with acetonitrile, *p*-nitrophenyl ester **17a** was dissolved in dimethylformamide and reacted with the specified alcohol or amine in the presence of Et₃N to provide the respective ester **19a** and amides **18a**, **21a–27a**, and **29a** after purification by flash chromatography (Scheme 5). Amide **34a** was synthesized from *p*-nitrobenzoyl

(36) Chica, R. A.; Gagnon, P.; Keillor, J. W.; Pelletier, J. N. Tissue transglutaminase acylation: proposed role of conserved active site Tyr and Trp residues revealed by molecular modelling of peptide substrate binding. *Protein Sci.* **2004**, *13*, 979–991.

(37) Gobec, S.; Sova, M.; Kristan, K.; Rižner, T. L. Cinnamic acid esters as potent inhibitors of fungal 17 β -hydroxysteroid dehydrogenase - a model enzyme of the short-chain dehydrogenase/reductase superfamily. *Bioorg. Med. Chem. Lett.* **2004**, *14*, 3933–3936.

(38) Penning, T. D.; Russell, M. A.; Chen, B. B.; Chen, H. Y.; Desai, B. N.; Docter, S. H.; Edwards, D. J.; Gesiki, G. J.; Freeman, S. K.; Hanneke, M. L.; Shannon, K. E.; Westlin, M. M.; Nickols, G. A. Synthesis of cinnamic acids and related isosteres as potent and selective α v β 3 receptor antagonists. *Bioorg. Med. Chem. Lett.* **2004**, *14*, 1471–1476.

(39) Adisakwattana, S.; Sookkongwareeb, K.; Roengsumran, S.; Petsom, A.; Ngamrojanavanich, N.; Chavasiri, W.; Deesamer, S.; Yibchok-anun, S. Structure–activity relationships of *trans*-cinnamic acid derivatives on α -glucosidase inhibition. *Bioorg. Med. Chem. Lett.* **2004**, *14*, 2893–2896.

(40) Bellamy, F. D.; Ou, K. Selective reduction of aromatic nitro compounds with stannous chloride in non acidic and non aqueous medium. *Tetrahedron Lett.* **1984**, *25*, 839–842.

(41) Nelson, A. T.; Houlihan, W. J., *The Aldol Condensation in Organic Reactions*. Wiley: New York, 1968; p 44.

(42) Gagnon, P.; Huang, X.; Therrien, E.; Keillor, J. W. Peptide Coupling of Unprotected Amino Acids Through In Situ *p*-Nitrophenyl Ester Formation. *Tetrahedron Lett.* **2002**, *43*, 7717–7719.

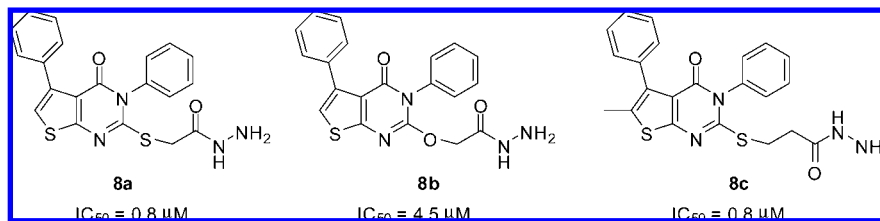


FIGURE 3. Representative structures of reversible transglutaminase inhibitors.³⁵

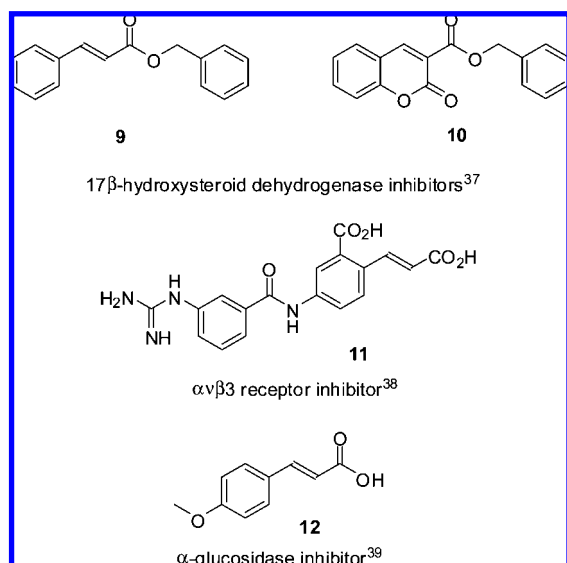


FIGURE 4. Structures of different *trans*-cinnamoyl derivative inhibitors.

chloride and benzotriazole using Et_3N in dichloromethane overnight at room temperature.

The coumarin derivative 3-((*E*)-3-(4-nitrophenyl)acryloyl)-2*H*-chromen-2-one (**28a**) was synthesized from treatment of *p*-nitrobenzaldehyde with 3-((triphenylphosphinyl)acetenyl)-coumarin (**36**) in toluene overnight at room temperature. Under these conditions, the product was found to precipitate and simple filtration provided the pure product as a yellow solid in 36% isolated yield. 3-((Triphenylphosphinyl)acetenyl)coumarin (**36**) was prepared from 3-((triphenylphosphimyl)acetyl)coumarin bromide (**35**) using potassium carbonate in 2:1 EtOH/ H_2O to give the product as a yellow crystalline solid after extraction, in 95% isolated yield. The required precursor **35** was prepared by nucleophilic displacement of 3-(bromoacetyl)coumarin with triphenylphosphine in dichloromethane, which gave a yellow crystalline solid in quantitative yield (Scheme 6).

Dienones **37a** and **38a** were synthesized from *p*-nitrocinnamaldehyde following protocols similar to those described above for the synthesis of the azachalcone and the benzotriazole derivatives from benzaldehydes (Scheme 7). Amide **37a** was thus obtained as a yellow solid in 48% yield and ketone **38a** as a yellow-orange solid in 33% yield.

Enzyme Inhibition. Recombinant guinea pig liver TGase was expressed in *Escherichia coli* and subsequently purified according to our previously reported procedure.⁴³ In addition to being easy to obtain in excellent yield and solubility, guinea pig liver TGase was chosen for this study because it shows 80%

homology with human tissue TGase⁴⁴ and may thus serve as a model for the evaluation of inhibitors of potential therapeutic utility.

The IC_{50} values of synthetic analogues **14a–38a** were determined from inhibition of the reaction of $54.4 \mu\text{M}$ of the chromogenic TGase substrate *N*-Cbz-Glu(γ -*p*-nitrophenyl ester)Gly with ~ 0.010 U of recombinant guinea pig liver TGase as previously reported⁴⁵ and described in detail in the Experimental Section. The mode of inhibition was determined for the representative lead compound **14a** through nonlinear regression of initial rate data to the Michaelis–Menten equation (Figure 6A). The apparent K_m value of the acyl-donor substrate increased with inhibitor concentration, while V_{max} remained constant (Figure 6B), indicating that cinnamoyl amide **14a** is a competitive inhibitor of the acyl-donor substrate used in the assay.

The structure–activity relationship study for TG2 inhibition by the cinnamoyl benzotriazolyl amides was initially focused on the effect of substituents on the cinnamoyl aromatic ring: *p*- NO_2 , *p*-MeO, *m*-MeO, *o*-MeO, *p*-Me, *m*-Me, *o*-Me, *p*-Cl, *o*-Cl, *p*-BOC NH , *m*-BOC NH , *p*-Fmoc NH , and *p*-MeO $_2\text{C}$ derivatives (**15a,d–i,k,m–p,q**) were synthesized and evaluated (Table 1). Among the analogues tested, the most potent TGase inhibitors (IC_{50} values between 18 and $74 \mu\text{M}$) possessed a substituent with an sp^2 -hybridized oxygen: *p*- NO_2 (**15a**), *p*- and *m*-BOC NH (**15n,o**), *p*-Fmoc NH (**15p**), and *p*-MeO $_2\text{C}$ (**15q**). Within this series, large substituents in the para position gave the best results. Analogues with other ring substituents (i.e., Me–, MeO–, and Cl–) exhibited lower potency in the inhibition assay. This may in part be due to their limited solubility. The position of these ring substituents did not influence inhibitor potency, and no trend was observed with respect to the electron-withdrawing nature of the substituent. Although this series was constructed to investigate the potential importance of a putative aromatic dipole effect, no correlation was observed to support this hypothesis. Rather, the observed affinities were interpreted to be due to specific interactions from the substituents themselves.

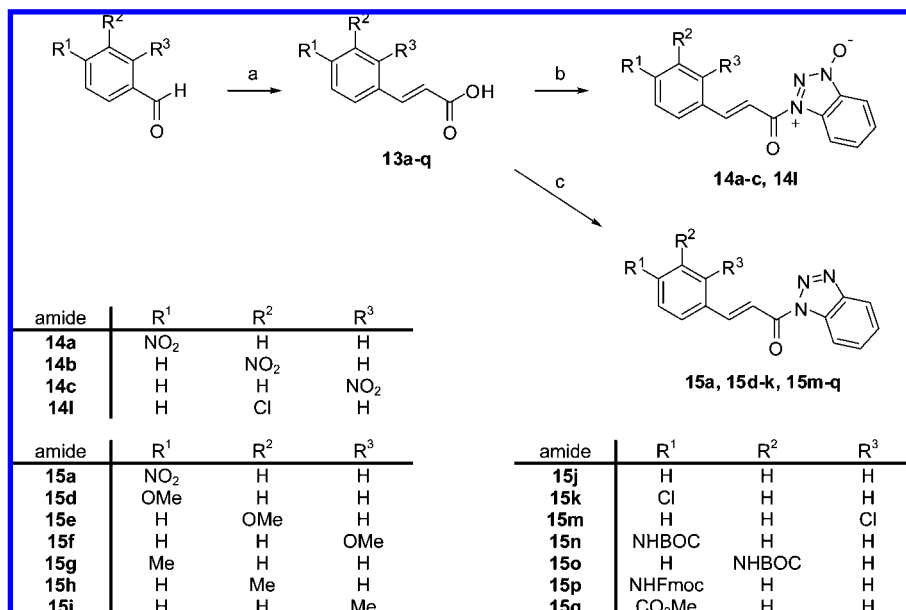
A particularly potent group of inhibitors were the cinnamoyl oxybenzotriazolyl amides (**14a–c,i**). Comparison of the inhibitory activity of the *p*-, *m*-, and *o*- NO_2 cinnamoyl oxybenzotriazolyl amides **14a–c** (Table 1) demonstrated that substitution at the ortho position resulted in decreased activity. In marked difference from the case for the chlorinated benzotriazolyl derivatives **15k,m**, *m*-chloro cinnamoyl oxybenzotriazolyl amide **14l** exhibited an IC_{50} value of $41 \mu\text{M}$ despite not having an sp^2 -hybridized oxygen (Table 1).

The importance of the cinnamate double bond for activity (Table 2) was demonstrated by the significant loss of activity of analogues **32a** and **33a**, wherein the phenylvinyl group of

(43) Gillet, S. M. F. G.; Chica, R. A.; Keillor, J. W.; Pelletier, J. N. Expression in *Escherichia coli* and Purification of Hexahistidine-Tagged Guinea Pig Liver Transglutaminase. *Prot. Exp. Purif.* **2004**, *33*, 256–264.

(44) Aeschlimann, D.; Paulsson, M. Transglutaminases: protein cross-linking enzymes in tissues and body fluids. *Thromb. Haemost.* **1994**, *71*, 402–415.

(45) Leblanc, A.; Gravel, C.; Labelle, J.; Keillor, J. W. Kinetic Studies of Guinea Pig Liver Transglutaminase Reveal a General Base Catalyzed Deacylation Mechanism. *Biochemistry* **2001**, *40*, 8335–8342.

SCHEME 2. Synthesis of the Substituted Cinnamoyl Benzotriazolyl Amides and Oxybenzotriazolyl Amides^a

^a In this and all following schemes, compounds are numbered according to the acylated moiety and lettered according to the aryl (acyl) substitution pattern. Reagents and conditions: (a) (i) Ph₃PCH₂CO₂-*t*-BuBr, KHMDS, THF, 1 h, room temperature, (ii) TFA/CH₂Cl₂, 4 h, 4 °C, 37–74%; (b) hydroxybenzotriazole, DIC, DMAP, DMF, 16 h, room temperature, 52–64%; (c) benzotriazole, DIC, DMAP, DMF, 16 h, room temperature, 12–70%.

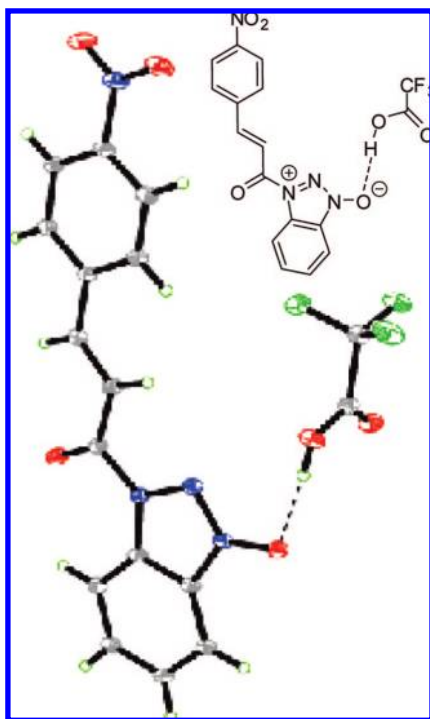
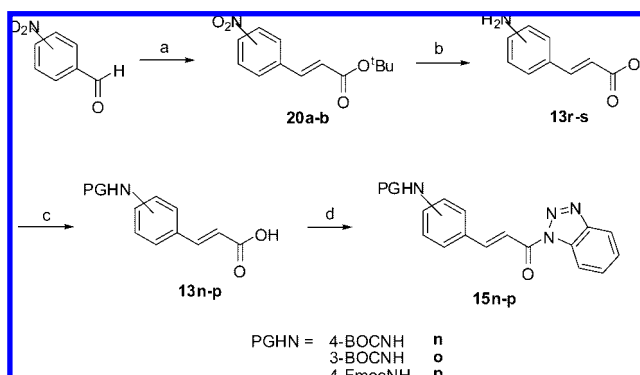
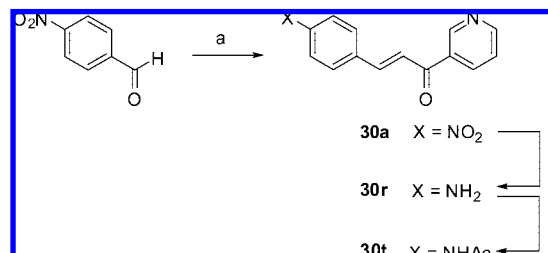


FIGURE 5. X-ray structure of *p*-nitrocinnamoyl oxybenzotriazolyl amide **14a** with trifluoroacetic acid.

15a is reduced to a phenylethyl group or replaced by a benzyloxy group, respectively. On complete removal of the double bond, *p*-nitrobenzoyl benzotriazolyl amide **34a** was found to react in a time-dependent fashion as an irreversible inhibitor, possibly due to acylation of an amino acid moiety with loss of the benzotriazole leaving group. Taken together, these results suggested that the extended conjugation and conformational rigidity of the amide were important for reversible inhibitory activity. Finally, the importance of the distance between the two aromatic moieties of these inhibitors was evaluated. Namely,

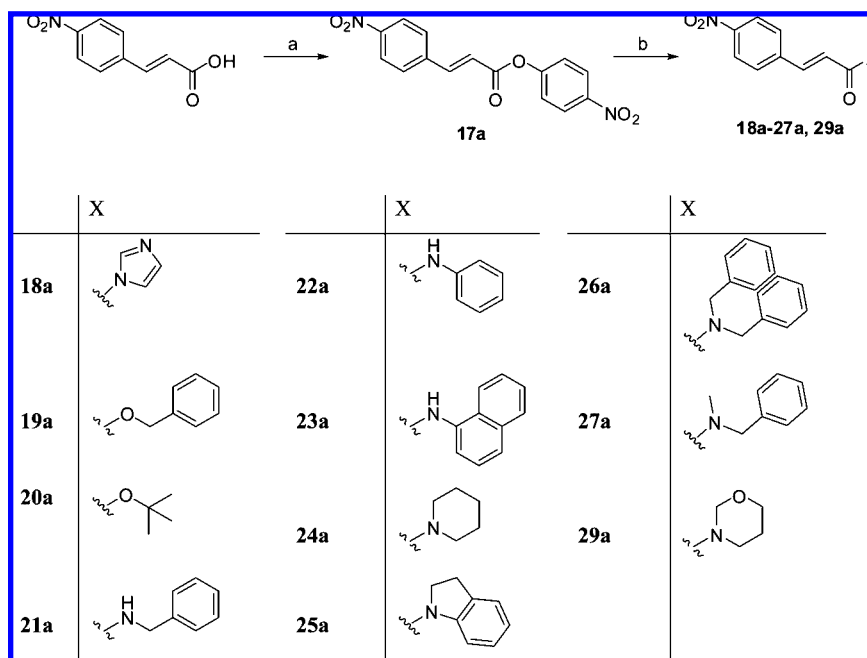
SCHEME 3. Synthesis of the Amide-Substituted Cinnamoyl Benzotriazolyl Amides^a

^a Reagents and conditions: (a) Ph₃PCH₂CO₂-*t*-BuBr, KHMDS, THF, 1 h, room temperature, 37–74%; (b) (i) SnCl₂, EtOH, 30 min, 70 °C, (ii) TFA/CH₂Cl₂, 4 h, 4 °C, 64%; (c) (BOC)₂O, Et₃N, MeOH, 16 h, room temperature, 45%, or FmocCl, NaHCO₃, dioxane/H₂O 16 h, room temperature, 37%; (d) benzotriazole, DIC, DMAP, DMF, 16 h, room temperature, 12–61%.

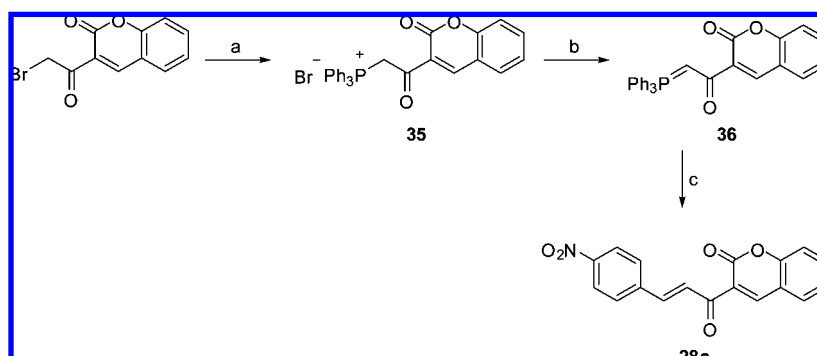
SCHEME 4. Synthesis of the Substituted Azachalcones^a

^a Reagents and conditions: (a) 3-acetylpyridine, KOH, MeOH/H₂O, 30 min, room temperature, 75%; (b) SnCl₂, EtOH, 30 min, 70 °C, 57%; (c) 40% (Ac)₂O/pyridine, 2 h, room temperature, 77%.

benzotriazole derivative **37a** and azachalcone **38a** were synthesized and tested as inhibitors bearing an additional double bond. Neither of these two extended conjugated compounds showed significant inhibition (IC₅₀ > 200 μM). Apparently, the

SCHEME 5. Synthesis of Different Amides and Esters of *p*-Nitrocinnamic Acid^a

^a Reagents and conditions: (a) *p*-nitrophenyl chloroformate, Et₃N, DMAP, CH₃CN, 1 h, room temperature, 94%; (b) amine or alcohol, Et₃N, DMAP, CH₃CN, 16 h, room temperature, 42–80%.

SCHEME 6. Synthesis of 3-((*E*)-3-(4-Nitrophenyl)acryloyl)-2*H*-chromen-2-one (28a)^a

^a Reagents and conditions: (a) PPh₃, CH₂Cl₂, 1.5 h, room temperature, 100%; (b) K₂CO₃ EtOH/H₂O, 1.5 h, room temperature, 95%; (c) *p*-nitrobenzaldehyde, toluene, 16 h, room temperature, 36%.

longer distance between the phenyl group and the benzotriazole nitrogen of compound **37a** is detrimental to affinity for TG2, in comparison to the shorter distance in the corresponding potent cinnamide **15a**.

Considering that the benzotriazolyl amides were potentially labile to nucleophilic attack and solvolysis, a series of more stable cinnamoyl amides and esters were evaluated (Table 3). Esters **19a** and **20a** showed little inhibitory activity, demonstrating at least that the amide moiety of this class of inhibitors is important for affinity. Secondary amides **21a**–**23a** also showed markedly less activity than the tertiary benzotriazole amides, suggesting initially that tertiary amides may show greater affinity than secondary amides. The lack of activity of piperidine and pyrrolidine amides **24a** and **25a** indicated, however, that recognition required more than just a tertiary amide group. Amides **24a** and **25a** differed from the benzotriazole series by their lack of an aromatic ring and additional nitrogen atoms in the ring. Inhibitory activity was observed when the benzotriazole was replaced by other heterocycles containing multiple hydrogen bond acceptors such as benzotriazolides **14a**, **15a**, and **16a** and

imidazolidine **18a**. In addition, the tertiary dibenzyl amide **26a** exhibited an IC₅₀ value of 57 μM, indicating that other factors may contribute to enzyme affinity.

Considering that the triazole nitrogens may serve as hydrogen bond acceptors in the enzyme-bound structure, a second subclass of cinnamoyl derivatives was designed, in which this moiety was replaced by a 3-pyridine group. Azachalcones **30a,r,t** proved to be as effective as the benzotriazolyl amide inhibitors (Table 1) and relatively more soluble in the 5% DMF/95% H₂O solvent mixture used for the enzymatic assay. Furthermore, the presence of the nitrogen in the azachalcones was demonstrated to be important for TG2 inhibition, by lack of activity of the parent chalcone, (*E*)-3-(4-nitrophenyl)-1-phenylprop-2-en-1-one. In this series the importance of the *p*-nitro group on the cinnamyl ring was also probed. Reduction to the (*E*)-3-(4-aminophenyl)-1-phenylprop-2-en-1-one **30r** resulted in a 5-fold loss of potency, which was recovered by acylation of the pendant amino group in acetamide **30t** (Table 1). This observation reinforces the notion that an sp² hybridized oxygen extending from the para

TABLE 1. Influence of the Cinnamoyl Aromatic Substituent

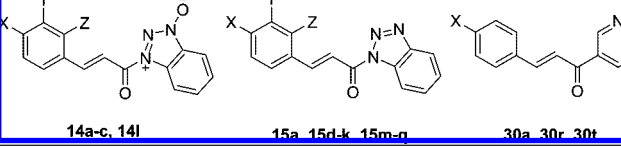
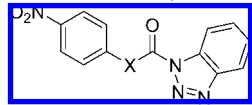
				
compd	X	Y	Z	IC ₅₀ (μM)
14a	NO ₂	H	H	43 ± 2
14b	H	NO ₂	H	24 ± 5
14c	H	H	NO ₂	>100
14l	H	Cl	H	41 ± 9
15a	NO ₂	H	H	74 ± 15
15d	MeO	H	H	>100
15e	H	MeO	H	>100
15f	H	H	MeO	>100
15g	Me	H	H	>100
15h	H	Me	H	>100
15i	H	H	Me	>100
15j	H	H	H	>100
15k	Cl	H	H	>100
15m	H	H	Cl	>100
15n	BOCNH	H	H	18 ± 1
15o	H	BOCNH	H	39 ± 2
15p	FmocNH	H	H	25 ± 5
15q	MeO ₂ C	H	H	27 ± 4
30a	NO ₂	H	H	21 ± 4
30r	NH ₂	H	H	148 ± 27
30t	AcNH	H	H	28 ± 4

TABLE 2. Influence of the Cinnamoyl Double Bond

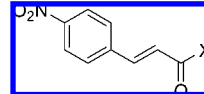
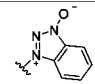
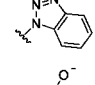
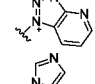
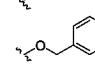
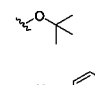
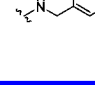
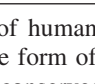
		
compd	X	IC ₅₀ (μM)
15a	CH=CH	74 ± 15
32a	CH ₂ -O	>200
33a	CH ₂ -CH ₂	>200
34a		irreversible
37a	CH=CHCH=CH	>200

position may pick up favorable interactions with the enzyme, increasing binding affinity.

To further test the hypothesis that the triazole nitrogens increased affinity by serving as hydrogen bond acceptors, coumarin derivative **28a** was synthesized and evaluated. Coumarin **28a**, which contains two oxygens capable of serving as hydrogen bond acceptors, exhibited an IC₅₀ value of 48 μM (Table 3). Considering that a potential hydrogen bond acceptor (N or O) was important for the affinity of the acylated moiety, the influence of aromaticity was probed. Amide **29a**, possessing an 1,3-oxazinan-3-yl moiety, was synthesized and exhibited little inhibitory potency, suggesting that aromaticity (or at least planarity) of the acylated ring was critical.

In light of their ability to compete with donor substrate, the cinnamoyl inhibitors may be considered to interact with the acyl-donor substrate binding site. (However, it is important to note that steady-state kinetic data alone do not distinguish between alternative binding modes, such as at the tightly coupled nucleotide binding site.⁴⁶) In the published structures of the extended, acylated form⁴⁷ as well as the compact, inactive

TABLE 3. Influence of the Acylated Moiety

				
Compd	X	IC ₅₀ (μM)	Compd	IC ₅₀ (μM)
14a		43 ± 2	22a	> 200
15a		74 ± 5	23a	> 200
16a		33 ± 2	24a	> 200
18a		45 ± 10	25a	> 200
19a		> 200	26a	57 ± 7
20a		> 200	27a	> 200
21a		> 200	28a	48 ± 6
			29a	> 200

form⁴⁸ of human TG2, the acyl-donor substrate binding site takes the form of a shallow hydrophobic groove. This groove is also conserved in the highly homologous red sea bream TG2.^{36,49} Binding of the aromatic ring(s) of our cinnamoyl inhibitors in this hydrophobic groove would block access to the active site.³⁶ The restricted and hydrophobic nature of this pocket may explain why voluminous nonplanar rings do not appear to be accommodated at this position (e.g., **29a**) and why longer rigid compounds (e.g., **37a** and **38a**) would incur unfavorable steric hindrance.

To examine the enzyme selectivity of this new family of TG2 inhibitors, several representative compounds (**14a**, **15p**, **18a**, **28a**, and **30a**) were further tested as inhibitors of related enzymes. For these studies, Factor XIIIa was chosen because it is a member of the family of transglutaminase enzymes and its inhibition *in vivo* may lead to compromised coagulation and toxicity. Caspase 3 was also chosen because, as a cysteine protease, its acyl transfer mechanism is phenomenologically similar to that of TGase. At concentrations approaching the limits of their solubility, most of those compounds had no discernible effect on the activities of either of these enzymes (see the Supporting Information). Only the coumarin derivative **28a** was found to display slight inhibitory activity toward caspase 3—namely, 28% inhibition at 6 μM. This selectivity bodes well for *in vivo* application; evaluation of the efficacy of select compounds in cell culture is currently underway.

Summary

Novel trans-cinnamoyl derivatives have been synthesized and discovered to be reversible inhibitors of TG2, competitive with

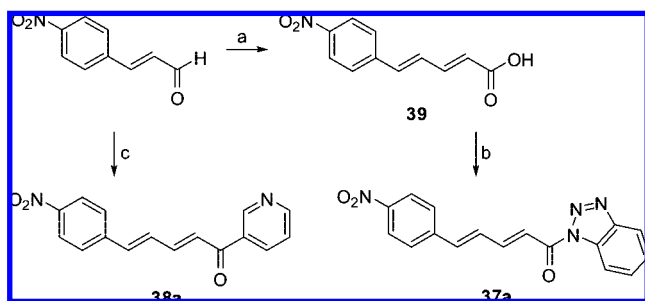
(46) Case, A.; Stein, R. L. Kinetic Analysis of the Interaction of Tissue Transglutaminase with a Nonpeptidic Slow-Binding Inhibitor. *Biochemistry* **2007**, *46*, 1106–1115.

(47) Pinkas, D. M.; Strop, P.; Brunger, A. T.; Khosla, C. Transglutaminase 2 undergoes a large conformational change upon activation. *PLoS Biol.* **2007**, *5*, e327.

(48) Liu, S.; Cerione, R. A.; Clardy, J. Structural basis for the guanine nucleotide-binding activity of tissue transglutaminase and its regulation of transamidation activity. *Proc. Natl. Acad. Sci. U.S.A.* **2002**, *99*, 2743–2747.

(49) Nogushi, K.; Ishikawa, K.; Yokoyama, K.-I.; Ohtsuka, T.; Nio, N.; Suzuki, E.-I. Crystal Structure of Red Sea Bream Transglutaminase. *J. Biol. Chem.* **2001**, *276*, 12055–12059.

SCHEME 7. Synthesis of (2*E*,4*E*)-5-(4-Nitrophenyl)penta-2,4-dienoyl Benzotriazolyl Amide (**37a**) and (2*E*,4*E*)-5-(4-Nitrophenyl)-1-(pyridin-3-yl)penta-2,4-dien-1-one (**38a**)^a



^a Reagents and conditions: (a) (i) $\text{Ph}_3\text{PCH}_2\text{CO}_2\text{-}t\text{-BuBr}$, KHMDS, THF, 1 h, room temperature, (ii) TFA/ CH_2Cl_2 , 4 h, 4 °C, 82%; (b) benzotriazole, DIC, DMAP, DMF, 16 h, room temperature, 48%; (c) 3-acetylpyridine, KOH, MeOH/ H_2O , 30 min, room temperature, 64%.

acyl-donor substrate. Among these derivatives, the most effective inhibitors were found to be the cinnamoyl benzotriazolyl amides and the 3-(substituted cinnamoyl)pyridines. Within these subclasses, it was noted that the most potent inhibitors possess para substituents containing an sp^2 -hybridized oxygen, maintain the distance and conjugation of the cinnamic double bond, and present acylated heterocycles that are able to serve as H-bond acceptors. We hypothesize that these inhibitors are bound in the hydrophobic groove of the acyl-donor binding site; modeling studies are underway that will guide the design of future inhibitors. Representative examples of the most potent inhibitors were found to be selective for TG2 with respect to related enzymes, which bodes well for future application in vivo.

Experimental Section

Kinetic Methods. Kinetic runs were recorded on a UV–visible spectrophotometer at 405 nm and 25 °C, in a buffer composed of 50 mM CaCl_2 , 50 μM EDTA, and 0.1 M MOPS (pH 7.0). All aqueous solutions were prepared using deionized water. All kinetic assays were carried out using 900 μL of buffer, 50 μL of 0.15 mg/mL TGase, and 25 μL of a 2.2 mM stock solution of substrate *N*-Cbz-Glu(γ -*p*-nitrophenyl ester)Gly, in the presence of 0–25 μL (contingent on solubility) of an anhydrous DMF stock solution of the inhibitor. Final inhibitor concentrations thus ranged from 1.8 μM to the solubility limit of each compound. Factor XIIIa activity was measured using a coupled-enzyme assay.⁵⁰ Factor XIIIa was added to a final concentration of 0.89 $\mu\text{g}/\text{mL}$ to a pH 8.5 solution (0.1 M Tris-HCl, 5 mM CaCl_2 , and 10 mM DDT) of 0.5 mM β -NADH, 3.3 mM *N*- α -acetyl-L-lysine methyl ester, 10 mM α -ketoglutaric acid sodium salt, and 297 $\mu\text{g}/\text{mL}$ glutamate dehydrogenase (GDH). The subsequent absorbance decrease was followed at 340 nm at 37 °C. Caspase 3 activity was measured by monitoring the release of *p*-nitroaniline (pNA) ($\lambda_{\text{abs}} = 405 \text{ nm}$) from the peptidic substrate Ac-Asp-Glu-Val-Asp-pNA (20 μM) catalyzed by human caspase 3 (250 ng/mL) at pH 7.4 (18.6 mM HEPES, 1.9 mM EDTA, 0.09% CHAPS, and 4.7 mM DTT).

Synthetic Methods. General Procedure A: Synthesis of *trans*-Cinnamoyl Benzotriazolyl Amides. *trans*-Cinnamic acid (0.1 mmol) was dissolved in 2 mL of DMF, treated with DIC (0.25 mmol) and benzotriazole (0.25 mmol), and stirred overnight. In the case of **15a**, **14a–c,g,k–q**, **16a**, and **37a**, the products precipitated and were collected by filtration and washed with 20 mL of diethyl ether. For **15d–f,h–j** and **33a**, the reaction mixture was diluted with 30 mL of EtOAc and washed with $3 \times 5 \text{ mL}$ of 1 N HCl, $3 \times 5 \text{ mL}$

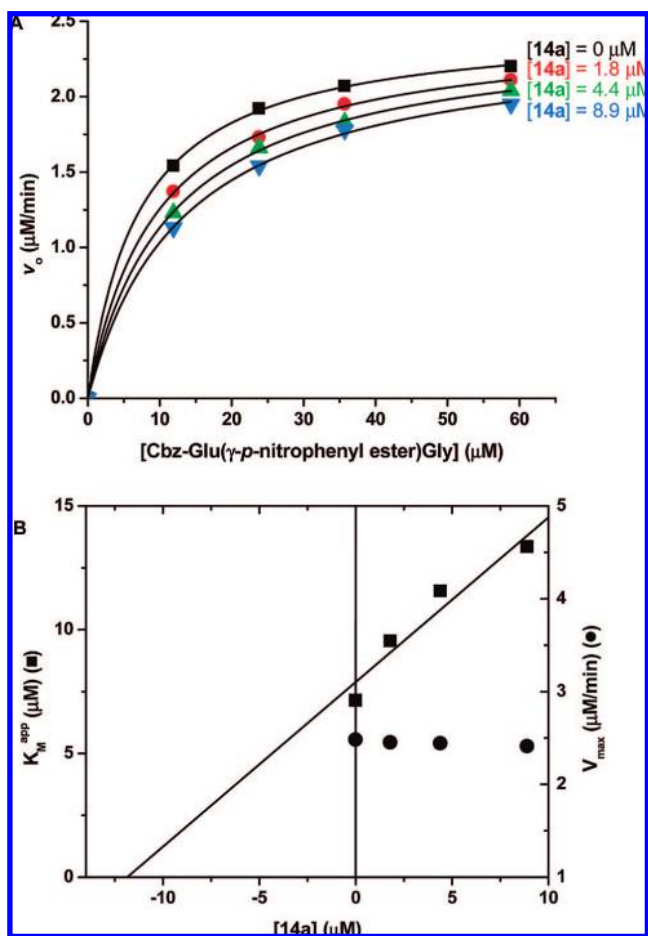


FIGURE 6. Competitive inhibition by cinnamoyl amide **14a**: (A) Michaelis–Menten plot of inhibition kinetic data; (B) replot showing independence of V_{max} values.

of 1 N NaOH, and $1 \times 10 \text{ mL}$ of brine. The organic layer was dried with MgSO_4 , filtered, and evaporated. The solid was recrystallized from EtOH (**15d,j**) or purified by flash chromatography (**15e,f,h,i** and **33a**).

General Procedure B: Synthesis of Substituted *trans*-Cinnamic Acids. In 3 mL of THF, ((*tert*-butoxycarbonyl)methyl)triphenylphosphonium bromide (0.33 mmol) and KHMDS (0.297 mmol) were dissolved and treated dropwise with a solution of the substituted benzaldehyde (0.165 mmol) in 1 mL of THF. After it was stirred for 1 h, the reaction mixture was washed twice with 2 mL of saturated NH_4Cl , dried with MgSO_4 , and evaporated to a residue that was passed through a short silica gel column (10 cm), with EtOAc as eluent. The collected fractions were evaporated, and the residue was dissolved in a minimum volume of DCM, cooled to 0 °C, and treated with a 2 mL aliquot of TFA. After the mixture was stirred for 4 h at 0 °C, the volatiles were removed by azeotropic evaporation from a mixture of cyclohexane and acetone. The solid product thus obtained was triturated with ether and filtered.

General Procedure C: Aldol Condensation. 3-Acetylpyridine (0.5 mmol) was dissolved in a 1:1 $\text{H}_2\text{O}/\text{MeOH}$ mixture (4 mL), and this solution was treated with the substituted benzaldehyde (1.5 mmol) and KOH (1.5 mmol), stirred for 30 min, and filtered. The precipitated product, which was collected by filtration, was washed with a minimum amount of ethanol.

General Procedure D: Nitro Group Reduction with Tin(II) Chloride. The nitro aromatic analogue (1 mmol) was dissolved in 5 mL of absolute ethanol, and this solution was treated with $\text{SnCl}_2 \cdot 2\text{H}_2\text{O}$ (5 mmol), heated to 70 °C, stirred for 30 min under N_2 , treated with 30 mL of water, and neutralized with a solution of 5% NaHCO_3 . The aqueous phase was extracted with $3 \times 20 \text{ mL}$

(50) Day, N.; Keillor, J. W. A Continuous Spectrophotometric Linked-Enzyme Assay for Transglutaminase Mediated Transpeptidation Activity. *Anal. Biochem.* **1999**, 274, 141–144.

of EtOAc. The combined organic phase was dried, filtered, and evaporated to a residue that was purified by chromatography on silica gel with EtOAc as eluant.

General Procedure E: Synthesis of Amides and Esters of *p*-Nitrocinnamic Acid. *p*-Nitrocinnamoyl *p*-nitrophenyl ester (**46**; 0.16 mmol) was dissolved in 2 mL of CH₂Cl₂, and this solution was treated with the specified alcohol or amine (0.18 mmol) using Et₃N (0.48 mmol) as base. After the mixture was stirred overnight at room temperature, the volatiles were removed and the resulting mixture was diluted with 30 mL of EtOAc. The organic phase was washed with 3 × 6 mL of 0.1 N HCl, 8 × 6 mL of 1 N NaOH, and 2 × 5 mL of brine, dried with MgSO₄, filtered, and evaporated to a residue that was triturated with diethyl ether to give a solid.

***m*-Nitrocinnamic Acid (**13b**).** Acid **13b** was prepared from *m*-nitrobenzaldehyde using general procedure B and isolated as a pale yellow solid (74% yield). Mp: 200–202 °C. ¹H NMR (*d*₆-DMSO): δ 8.50 (s, 1H), 8.21 (dd, 1H, *J* = 8.2, 1.7 Hz), 8.17 (d, 1H, *J* = 8.0 Hz), 7.69 (m, 2H), 6.73 (d, 1H, *J* = 15.8 Hz). ¹³C NMR (*d*₆-DMSO): δ 158.0, 140.6, 134.4, 129.4, 127.5, 124.1, 118.6, 117.2, 116.7. HRMS (ESI): *m/z*: *m/z* calcd for C₉H₆NO₄ ([M – H][–]) 192.0302, found 192.0310.

***p*-Aminocinnamic Acid (**13r**).** Acid **13r** was prepared using general procedure D from the ester **20a** to give a product that was diluted in a minimum of CH₂Cl₂ and treated with TFA (3 mL) at 0 °C for 4 h. The volatiles were removed under vacuum, and the product was triturated with diethyl ether to give an orange solid (64% yield). Mp: 265–267 °C dec. ¹H NMR (CD₃OD): δ 7.73 (d, 2H, *J* = 8.5 Hz), 7.67 (d, 1H, *J* = 16.1 Hz), 7.40 (d, 2H, *J* = 8.5 Hz), 6.52 (d, 1H, *J* = 16.0 Hz). ¹³C NMR (CD₃OD): δ 161.1, 137.5, 130.5, 127.6, 125.1, 119.6, 116.5. HRMS (ESI): *m/z* calcd for C₉H₉NO₂ ([M + H]⁺) 164.0706, found 164.0709.

***p*-((*tert*-Butoxycarbonyl)amino)cinnamic Acid (**13n**).** Acid **13n** (0.5 mmol) was dissolved in 5 mL of a dioxane/H₂O (1:1) solution, and this solution was treated with di-*tert*-butyl dicarbonate ((BOC)₂O) (0.6 mmol) and solid NaHCO₃ (5 mmol), stirred overnight at room temperature, and evaporated to a residue that was diluted with 40 mL of 1 N NaOH. The aqueous phase was washed with 3 × 10 mL of CH₂Cl₂ and neutralized with 1 N HCl. The acid was extracted with 3 × 10 mL of EtOAc. The combined organic phase was dried with MgSO₄ and filtered. The volatiles were removed, and the product was obtained without further purification as a white solid (45% yield). Mp: 195–197 °C dec. ¹H NMR (CD₃OD): δ 7.61 (d, 1H, *J* = 16.0 Hz), 7.47 (d, 4H, *J* = 5.4 Hz), 6.35 (d, 1H, *J* = 15.9 Hz), 1.51 (s, 9H). ¹³C NMR (CD₃OD): δ 171.6, 155.7, 147.0, 143.7, 130.9, 130.7, 120.3, 117.8, 82.0, 29.5. HRMS (ESI): *m/z* calcd for C₁₄H₁₇NO₄Na ([M + Na]⁺) 286.1050, found 286.1045.

***p*-(((9-Fluorenylmethoxy)carbonyl)amino)cinnamic Acid (**13p**).** Acid **13r** (0.5 mmol) was dissolved in 5 mL of a dioxane/H₂O (1:1) solution, and this solution was treated with (9-fluorenylmethoxy)carbonyl chloride (Fmoc-Cl; 0.6 mmol) using NaHCO₃ (5 mmol) as base. The mixture was stirred overnight at room temperature. Then the solvent was reduced and the residue was diluted in 40 mL of water. The aqueous phase was acidified with 6 N HCl. The acid was extracted with 3 × 10 mL of EtOAc. The organic phase was dried with MgSO₄ and filtered. The solvent was removed and the product obtained after trituration with diethyl ether as an orange solid (37% yield). Mp: 270–272 °C dec. ¹H NMR (*d*₆-DMSO): δ 9.92 (s, 1H), 7.90 (d, 2H, *J* = 7.3 Hz), 7.73 (d, 2H, *J* = 7.4 Hz), 7.45 (m, 9H), 6.37 (d, 1H, *J* = 16.0 Hz), 4.50 (d, 2H, *J* = 6.4 Hz), 4.30 (t, 1H, *J* = 6.4 Hz). ¹³C NMR (*d*₆-DMSO): δ 158.6, 145.2, 136.4, 136.4, 133.9, 133.8, 123.0, 122.3, 121.7, 121.2, 119.3, 114.8, 112.9, 111.9, 64.6, 47.0. HRMS (ESI): *m/z* calcd for C₂₄H₂₀NO₄ ([M + H]⁺) 386.1387, found 386.1383.

***p*-Nitrocinnamoyl Oxybenzotriazolyl Amide (**14a**).** Amide **14a** was prepared from *p*-nitrocinnamic acid using general procedure A and isolated as a pale yellow solid (55% yield). Mp: 212–214 °C dec. ¹H NMR (*d*₆-DMSO): δ 8.28 (d, 2H, *J* = 8.8 Hz), 8.02 (d, 3H, *J* = 8.6 Hz), 7.75 (d, 1H, *J* = 8.3 Hz), 7.68 (d, 1H, *J* = 16.1

Hz), 7.58 (t, 1H, *J* = 6.9 Hz), 7.46 (t, 1H, *J* = 8.2 Hz), 6.78 (d, 1H, *J* = 16.1 Hz). Anal. Calcd for C₁₅H₁₀N₄O₄: C, 58.07; H, 3.25; N, 18.06. Found: C, 59.23; H, 3.35; N, 19.16. The structure of the trifluoroacetate salt of **14a**, which was crystallized in TFA, was solved at the Université de Montréal X-ray facility using direct methods (SHELXS 97) and refined with SHELXL 97: C₁₅H₁₀N₄O₄·C₂HF₃O₂; *M*_r = 424.30; triclinic, colorless crystal; space group *P*1; unit cell dimensions *a* = 7.7137(2) Å, *b* = 9.7911(2) Å, *c* = 12.1711(2) Å, α = 96.2560(10)°, β = 107.4280(10)°, γ = 96.4560(10)°; volume of unit cell 861.55(3) Å³; *Z* = 2.

***p*-Nitrocinnamoyl Benzotriazolyl Amide (**15a**).** Amide **15a** was prepared from *p*-nitrocinnamic acid using general procedure A and isolated as a pale yellow solid (70% yield). Mp: 213–215 °C. ¹H NMR (*d*₆-DMSO): δ 8.27 (m, 8H), 7.81 (t, 1H, *J* = 7.2 Hz), 7.64 (t, 1H, *J* = 7.2 Hz). ¹³C NMR (*d*₆-DMSO): δ 168.1, 149.0, 142.4, 141.8, 139.7, 131.3, 130.4, 130.2, 126.4, 125.2, 125.0, 124.7, 115.9. HRMS (ESI): *m/z* calcd for C₁₅H₁₁N₄O₃ ([M + H]⁺) 295.0826, found 295.0816.

***p*-Nitrocinnamoyl *p*-Nitrophenyl Ester (**17a**).** Ester **17a** was prepared by treating *p*-nitrocinnamic acid (1 mmol) in acetonitrile (6 mL) with Et₃N (1 mmol) and DMAP (0.1 mmol) at room temperature for 5 min, followed by addition of *p*-nitrophenyl chloroformate (1.1 mmol) and stirring for 1 h. The precipitate was filtered and washed with 5 mL of acetonitrile, which gave a pale yellow solid (94% yield). Mp: 181–183 °C. ¹H NMR (CDCl₃): δ 8.32 (d, 2H, *J* = 9.1 Hz), 8.27 (d, 2H, *J* = 8.8 Hz), 8.10 (d, 2H, *J* = 8.9 Hz), 8.02 (d, 1H, *J* = 16.1 Hz), 7.54 (d, 2H, *J* = 9.1 Hz), 7.13 (d, 1H, *J* = 16.1 Hz). ¹³C NMR (*d*₆-DMSO): δ 164.7, 156.2, 149.3, 146.1, 145.5, 141.0, 130.8, 126.3, 125.0, 124.2, 121.8. HRMS (ESI): *m/z* calcd for C₁₅H₁₀N₂O₆Ag ([M + Ag]⁺) 420.9584, found 420.9589.

***p*-Nitrocinnamoyl Imidazolyl Amide (**18a**).** Amide **18a** was prepared using general procedure E, from imidazole in acetone, to give a white solid (68% yield). Mp: 178–179 °C dec. ¹H NMR (*d*₆-DMSO): δ 8.82 (s, 1H), 8.32 (d, 2H, *J* = 8.9 Hz), 8.20 (d, 2H, *J* = 8.9 Hz), 8.09 (d, 1H, *J* = 15.6 Hz), 7.96 (t, 1H, *J* = 1.31 Hz), 7.85 (d, 1H, *J* = 15.5 Hz), 7.17 (t, 1H, *J* = 0.9 Hz). ¹³C NMR (*d*₆-DMSO): δ 158.0, 140.3, 134.1, 133.7, 128.5, 124.0, 123.1, 118.3, 118.2, 118.1. HRMS (ESI): *m/z* calcd for C₁₂H₁₀N₃O₃ ([M + H]⁺) 244.0717, found 244.0727.

***p*-Nitrocinnamoyl *tert*-Butyl Ester (**20a**).** ((*tert*-Butoxycarbonyl)methyl)triphenylphosphonium bromide (0.33 mmol) and KH-MDS (0.297 mmol) were dissolved in 3 mL of THF. *p*-Nitrobenzaldehyde (0.165 mmol) was dissolved in 1 mL of THF and added dropwise to the ylide suspension. The mixture was stirred for 1 h. The organic phase was then treated twice with 2 mL of saturated NH₄Cl and dried with MgSO₄, and the volatiles were removed by rotary evaporation. The product was purified by chromatography with EtOAc/hexane (20:80) as eluant to give a pale yellow solid (75% yield). Mp: 146–148 °C. ¹H NMR (CDCl₃): δ 8.21 (d, 2H, *J* = 8.9 Hz), 7.63 (d, 2H, *J* = 8.9 Hz), 7.60 (d, 1H, *J* = 16.1 Hz), 6.47 (d, 1H, *J* = 16.0 Hz), 1.52 (s, 9H). ¹³C NMR (CDCl₃): δ 165.6, 148.6, 141.1, 140.9, 128.8, 124.8, 124.4, 81.6, 28.4. HRMS (ESI): *m/z* calcd for C₁₃H₁₅NO₄Na ([M + Na]⁺) 272.0893, found 272.0895.

3-((*E*)-3-(4-Nitrophenyl)acryloyl)-2H-chromen-2-one (28a**).** Coumarin **36** (1 mmol) was dissolved in 10 mL of toluene, and this solution was treated dropwise with *p*-nitrobenzaldehyde (0.67 mmol) in 5 mL of toluene and stirred overnight at room temperature. At this point a precipitate formed, which was filtered and washed with toluene to give a yellow solid (36% yield). Mp: 272–274 °C. ¹H NMR (*d*₆-DMSO): δ 8.73 (s, 1H), 8.30 (d, 2H, *J* = 8.8 Hz), 8.03 (d, 2H, *J* = 8.7 Hz), 7.97 (d, 1H, *J* = 6.7 Hz), 7.84 (s, 2H), 7.78 (t, 1H, *J* = 8.4 Hz), 7.51 (d, 1H, *J* = 8.4 Hz), 7.45 (t, 1H, *J* = 7.5 Hz). HRMS (ESI): *m/z* calcd for C₁₈H₁₂NO₅ ([M + H]⁺) 322.0710, found 322.0716.

(*E*)-3-(4-Nitrophenyl)-1-(pyridin-3-yl)prop-2-en-1-one (30a**).** Ketone **30a** was prepared using general procedure C from *p*-

nitrobenzaldehyde and obtained as a pale yellow solid (75% yield). Mp: 182–184 °C. ¹H NMR (CDCl₃): δ 9.23 (s, 1H), 8.82 (d, 1H, *J* = 3.7 Hz), 8.29 (m, 3H), 7.80 (m, 3H), 7.58 (d, 1H, *J* = 15.7 Hz), 7.48 (m, 1H). ¹³C NMR (CDCl₃): δ 188.7, 154.0, 150.1, 149.1, 143.0, 140.8, 136.3, 133.2, 129.5, 125.2, 124.6, 124.2. HRMS (ESI): *m/z* calcd for C₁₄H₁₁N₂O₃ ([M + H]⁺) 255.0764, found 255.0769.

(E)-3-(4-Aminophenyl)-1-(pyridin-3-yl)prop-2-en-1-one (30r). Ketone **30r** was prepared using general procedure D from azachalcone **30a** and obtained as pale orange solid (57% yield). Mp: 167–169 °C. ¹H NMR (CDCl₃): δ 9.18 (d, 1H, *J* = 1.6 Hz), 8.76 (dd, 1H, *J* = 4.8, 1.6 Hz), 8.25 (dt, 1H, *J* = 8.0, 1.9 Hz), 7.77 (d, 1H, *J* = 15.5 Hz), 7.46 (m, 3H), 7.28 (d, 1H, *J* = 15.5 Hz), 6.67 (d, 2H, *J* = 8.6 Hz), 4.07 (s, 2H). ¹³C NMR (CDCl₃): δ 180.5, 146.9, 144.3, 144.0, 141.5, 131.5, 129.9, 126.9, 121.0, 120.2, 114.1, 112.1. HRMS (ESI): *m/z* calcd for C₁₄H₁₃N₂O ([M + H]⁺) 225.1022, found 225.1027.

(E)-3-(4-(Acetylamino)phenyl)-1-(pyridin-3-yl)prop-2-en-1-one (30t). Ketone **30t** was prepared from aniline **30r** (0.045 mmol) and treated with 500 μL of a solution of 40% anhydrous acetic anhydride in pyridine at room temperature for 2 h. The solvent was removed, and the product was precipitated with 1 N NaOH. The solid was washed with water and obtained as a yellow solid (77% yield). Mp: 191–193 °C. ¹H NMR (CDCl₃): δ 9.21 (s, 1H), 8.79 (s, 1H), 8.27 (dt, 1H, *J* = 7.9 Hz, 1.8 Hz), 7.78 (d, 1H, *J* = 15.7 Hz), 7.59 (s, 4H), 7.39 (m, 3H), 2.19 (s, 3H). ¹³C NMR (CDCl₃): δ 189.4, 169.0, 153.4, 150.0, 145.8, 140.9, 136.3, 134.0, 130.1, 124.1, 120.5, 120.0, 25.1. HRMS (ESI): *m/z* calcd for C₁₆H₁₅N₂O₂ ([M + H]⁺) 267.1128, found 267.1141.

***p*-Nitrobenzoyloxycarbonylbenzotriazole (32a).** *p*-Nitrobenzyl chloroformate (0.5 mmol) was dissolved in 5 mL of CH₂Cl₂ and treated with benzotriazole (0.5 mmol) using Et₃N (2 mmol) as base. The mixture was stirred overnight at room temperature, diluted with CH₂Cl₂ (20 mL), and washed with 3 × 5 mL of 1 N HCl, 2 × 5 mL of 1 N NaOH, and 1 × 5 mL of brine. The organic phase was dried and filtered. The volatiles were removed, and the product was triturated with diethyl ether to provide a pale yellow solid (59% yield). Mp: 160–162 °C. ¹H NMR (CDCl₃): δ 8.27 (d, 1H, *J* = 8.9 Hz), 8.17 (m, 3H), 7.72 (d, 1H, *J* = 8.9 Hz), 7.65 (td, 1H, *J* = 8.3, 1.1 Hz), 7.53 (m, 2H), 5.26 (s, 2H). ¹³C NMR (CDCl₃): δ 154.8, 146.2, 142.3, 141.3, 132.0, 130.8, 128.8, 126.4, 124.2, 120.9, 113.6, 68.7. HRMS (ESI): *m/z* calcd for C₁₄H₁₁N₄O₄ ([M + H]⁺) 299.0775, found 299.0775.

***p*-Nitrobenzoyl Benzotriazolyl Amide (34a).** *p*-Nitrobenzoyl chloride (0.5 mmol) was dissolved in 5 mL of CH₂Cl₂ and treated with benzotriazole (0.5 mmol) and Et₃N (2 mmol). The mixture was stirred overnight at room temperature, diluted with CH₂Cl₂ (20 mL), washed with 3 × 5 mL of 1 N HCl, 2 × 5 mL of 1 N NaOH, and 1 × 5 mL of brine, dried over MgSO₄, and filtered. The volatiles were removed under reduced pressure, and the product was triturated with diethyl ether to give a white solid (49% yield). Mp: 194–196 °C. ¹H NMR (CDCl₃): δ 8.39 (m, 5H), 8.19 (dt, 1H, *J* = 8.3, 0.9 Hz), 7.75 (td, 1H, *J* = 8.2, 1.0 Hz), 7.60 (td, 1H, *J* = 8.2, 1.0 Hz). ¹³C NMR (CDCl₃): δ 165.3, 150.8, 146.2, 137.2, 133.0, 132.3, 131.4, 127.3, 123.8, 120.9, 115.1. HRMS (ESI): *m/z* calcd for C₁₃H₉N₄O₃ ([M + H]⁺) 269.0669, found 269.0676.

3-((Triphenylphosphinyl)acetyl)coumarin Bromide (35). Bromide **35** was synthesized from 3-(bromoacetyl)coumarin (2 mmol) in 5 mL of CH₂Cl₂ and triphenylphosphine (2 mmol). The mixture was stirred for 1.5 h at room temperature. The volatiles were

removed under reduced pressure. The crude product was triturated with diethyl ether, filtered, and washed again with diethyl ether to obtain a yellow crystalline solid (100% yield). Mp: 127–129 °C dec. ¹H NMR (CDCl₃): δ 9.24 (s, 1H), 7.83 (m, 6H), 7.60 (m, 1H), 7.23 (m, 2H), 6.35 (d, 2H, *J* = 12.2 Hz). ¹³C NMR: δ 189.2, 158.3, 155.4, 151.4, 135.1, 134.3, 133.8, 132.5, 131.5, 130.5, 130.2, 129.1, 125.4, 119.2, 118.0. HRMS (ESI): *m/z* calcd for C₂₉H₂₂O₃P ([M]⁺) 449.1379, found 449.1313.

3-((Triphenylphosphinyl)acetyl)coumarin (36). Bromide **35** (1 mmol) was dissolved in 4 mL of EtOH, treated dropwise with potassium carbonate (2 mmol) in 2 mL of H₂O, stirred for 1.5 h at room temperature, diluted with 40 mL of H₂O, and extracted with 4 × 10 mL of EtOAc. The combined organic phases were dried on MgSO₄, filtered, and evaporated under reduced pressure to give a yellow crystalline solid (95% yield). Mp: 114–116 °C dec. ¹H NMR (CDCl₃): δ 8.66 (s, 1H), 7.68 (m, 6H), 7.40 (m, 1H), 7.23 (d, 1H, *J* = 8.2 Hz), 7.14 (d, 1H, *J* = 7.4 Hz), 5.55 (d, 1H, *J* = 27.3 Hz). ¹³C NMR (CDCl₃): δ 168.4, 168.3, 154.1, 148.2, 138.0, 128.9, 128.0, 127.8, 127.7, 125.0, 123.0, 121.9, 120.6, 116.2, 113.0. HRMS (ESI): *m/z* calcd for C₂₉H₂₂O₃P ([M + H]⁺) 449.1301, found 449.1302.

***p*-(Methoxycarbonyl)benzaldehyde (40q).** 4-Carboxybenzaldehyde (2 mmol) was diluted in 6 mL of anhydrous MeOH. The mixture under N₂ was placed in an ice bath, and acetyl chloride (10 mmol) was added dropwise. The ice bath was removed, and the mixture was stirred overnight at room temperature. The methanol was removed under reduced pressure, and the mixture was diluted in 35 mL of EtOAc. The organic phase was washed with 5 × 10 mL of 1 N NaOH and 3 × 10 mL of brine, dried with MgSO₄, and filtered. The volatiles were removed, and the product was obtained as a pale yellow solid (96% yield). Mp: 142–144 °C. ¹H NMR (CDCl₃): δ 10.04 (s, 1H), 8.13 (d, 2H, *J* = 8.2 Hz), 7.89 (d, 2H, *J* = 8.1 Hz), 3.90 (s, 3H). ¹³C NMR (CDCl₃): δ 191.9, 166.3, 139.4, 135.3, 130.4, 129.7, 52.8. HRMS (ESI): *m/z* calcd for C₉H₉O₃ ([M + H]⁺) 165.0546, found 165.0543.

1,3-Oxazinane (41). 3-Aminopropanol (15 mmol) and formaldehyde (15 mmol) were diluted in 20 mL of anhydrous EtOH. The mixture was stirred under N₂ overnight at room temperature. EtOH was removed under reduced pressure, and the product was distilled (37–39 °C, 1.2 mmHg) to give the pure product as a colorless liquid (57% yield). ¹H NMR (CDCl₃): δ 4.29 (s, 2H), 3.79 (t, 2H, *J* = 5.3 Hz), 2.91 (t, 2H, *J* = 5.5 Hz), 1.50 (qu, 2H, *J* = 5.4 Hz). ¹³C NMR (CDCl₃): δ 80.1, 67.7, 44.1, 28.2. HRMS (ESI): *m/z* calcd for C₄H₁₀NO ([M + H]⁺) 88.0756, found 88.0760.

Acknowledgment. This work was supported financially by the Natural Sciences and Engineering Research Council of Canada (NSERC). C.P. is grateful to the Université de Montréal for a Bourse d'excellence.

Supporting Information Available: Text, tables, and figures giving details of the materials and general synthetic methods, additional compound data, kinetic data for TG2 selectivity, and ¹H and ¹³C NMR spectra and a CIF file giving X-ray data for structure **14a**. This material is available free of charge via the Internet at <http://pubs.acs.org>.

JO8004843